Characterization of the Tryptophan-Derived Quinone Cofactor of Methylamine Dehydrogenase by Resonance Raman Spectroscopy†

Gabriele Backes,‡ Victor L. Davidson,§ Fienke Huitema,‖ Johannis A. Duine,‖ and Joann Sanders-Loehr*,‡

Department of Chemical and Biological Sciences, Oregon Graduate Institute of Science and Technology, Beaverton, Oregon 97006-1999, Department of Biochemistry, University of Mississippi Medical Center, Jackson, Mississippi 39216-4505, and Department of Microbiology and Enzymology, Delft University of Technology, Julianalaan 67, 2628 BC Delft, The Netherlands

Received December 27, 1990; Revised Manuscript Received June 25, 1991

ABSTRACT: The resonance Raman (RR) spectrum of oxidized methylamine dehydrogenase ($MADH_{ox}$) exhibits a set of C–H, C–C, C=C, and C=O vibrational modes between 900 and 1700 cm^{-1} that are characteristic of the quinone moiety of the tryptophan tryptophylquinone (TTQ) cofactor. The close similarity of the RR spectra for MADHs from *Paracoccus denitrificans* (*Pd*), *Thiobacillus versutus* (*Tv*), and bacterium W3A1 proves that the same cofactor is present in all three proteins. The MADHs from *Pd* and *Tv* have a ν(C=O) mode at ~1625 cm^{-1} that shifts ~20 cm^{-1} upon ^{18}O substitution of one of the carbonyl oxygens and is assigned to the in-phase symmetric stretch of the two C=O groups. The semiquinone form of *Pd* MADH has its own characteristic RR spectrum with altered peak frequencies and intensities as well as a decrease in the total number of peaks. The hydroxide and ammonia adducts of $MADH_{ox}$ produce RR spectra similar to that of the semiquinone. The spectral changes in all three cases are interpreted as being due to reduced conjugation of the cofactor. The ammonia adduct is formulated as a carbinolamine, a likely intermediate in the enzymatic mechanism. In contrast, formation of the electron-transfer complex between amicyanin and $MADH_{ox}$ has no effect on the vibrational frequencies (and, hence, structure) of either the MADH quinone or the amicyanin blue copper site. The behavior of the TTQ cofactors of *Pd* and *Tv* MADHs are very similar to one another and somewhat different from W3A1 MADH, particularly with regard to adduct formation and ability to undergo isotope exchange with solvent. These differences are ascribed to the cofactor environments within the proteins rather than to the structure of the cofactor itself.

Methylamine dehydrogenase ($MADH_{ox}$) catalyzes the oxidation of methylamine to formaldehyde in a two-electron step via a covalently bound quinone cofactor [reviewed by Duine and Jongejan (1989)]. The blue copper protein amicyanin acts as the immediate electron acceptor for the reoxidation of the enzyme and mediates electron transfer from $MADH_{red}$ to a *c*-type cytochrome (Gray et al., 1988). The three best characterized MADHs from *Paracoccus denitrificans* (*Pd*) (Husain & Davidson, 1985), *Thiobacillus versutus* (*Tv*) (van Wielink et al., 1990), and a bacterium strain W3A1 (W3) (Kenney & McIntire, 1983) are tetrameric $\alpha_2\beta_2$ proteins with molecular weights of ~45 000 for the large subunit and ~15 000 for the small subunit. The crystal structure of *Tv* $MADH_{ox}$ confirms the tetrameric structure and shows that the cofactor is covalently bound within the small subunit but located in a hydrophobic channel between the large and small subunits (Vellieux et al., 1989).

For the past decade, MADH was considered to be a member of a large family of quinoproteins with a cofactor similar or identical to pyrroloquinoline quinone (PQQ) (de Beer et al., 1980; McIntire & Stults, 1986; van der Meer et al., 1987). Although PQQ has been proven to be the extractable cofactor in methanol dehydrogenase and glucose dehydrogenase from bacterial sources (Hartman & Klinman, 1988; Duine & Jongejan, 1989), recent results have challenged the idea of a universal quinone cofactor being present in all quinoproteins. In bovine plasma amine oxidase, the cofactor appears to be a derivatized tyrosyl residue, i.e., the quinone form of 2,4,5-trihydroxyphenylalanine or TOPA (Janes et al., 1990). In MADH, the modification of two amino acid residues was suggested by amino acid sequence analysis (Ishii et al., 1983) and subsequently confirmed by X-ray crystallography (Vellieux et al., 1989). However, the nature of the cofactor only became clear after the identification of these two residues as tryptophans in the DNA sequences for MADH from *Methylobacterium extorquens* AM1 (Chistoserdov et al., 1990) and *Tv* (Ubbink et al., 1991). NMR analyses of isolated cofactor-bearing peptides from W3 $MADH_{ox}$ suggest the tryptophan tryptophylquinone (TTQ) structure shown in Figure 1 where one of the indole rings has been oxidized to a quinone and is covalently attached to the indole of the other tryptophan moiety (McIntire et al., 1991b). This new structural model gives an excellent fit with the electron density maps obtained for $MADH_{ox}$ crystals from both *Tv* and *Pd* and indicates that TTQ is likely to be the correct structure (Chen et al., 1991). The TTQ redox cofactor in MADH is presumably formed via a posttranslational modification of one or both trytophan residues in the intact subunit.

Definitive proof for the existence of identical cofactors in the MADHs from the three different bacterial sources has been obtained by resonance Raman (RR) spectroscopy. Raman spectroscopy is a scattering technique that detects molecular vibrations. The resonance phenomenon leads to markedly enhanced intensities for the vibrational modes of atoms that are part of a chromophore (Nishimura et al., 1978; Carey, 1982). The set of conjugated double bonds in quinones leads to strong UV and visible absorption making quinone

† This research was supported by the National Institutes of Health, US Public Health Service, Grants GM-18865 (J.S.-L.) and GM-41574 (V.L.D.) and the Dutch Foundation of Chemical Research, SON (J. A.D.).

‡ Oregon Graduate Institute of Science and Technology.
§ University of Mississippi Medical Center.
‖ Delft University of Technology.

0006-2960/91/0430-9201$02.50/0

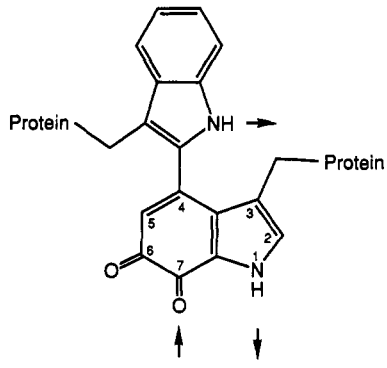

FIGURE 1: Proposed structure of tryptophan tryptophylquinone cofactor of $MADH_{ox}$ based on chemical analysis (McIntire et al., 1991a) and X-ray crystallography (Chen et al., 1991). The crystal structure also suggests that the cofactor is hydrogen bonded to the polypeptide backbone (indicated by arrows) and that the carbonyl at C-6 is more accessible to substrate.

species excellent subjects for RR spectroscopy (Nonaka et al., 1990). Derivatization of quinones with phenylhydrazines generates even stronger absorption bands and, thus, yields rich RR spectra for PQQ, amine oxidases, and MADH (Moog et al., 1986; Brown et al., 1991; McIntire et al., 1991a). Although these RR spectra are dominated by the phenylhydrazone moiety, they do show significant differences between amine oxidases and MADH, consistent with the proposed differences in quinone cofactor structures. However, the RR spectrum of the 2,4-dinitrophenylhydrazone derivative of PQQ is not well-distinguished from that of the plasma amine oxidase derivative, despite the marked structural differences in the quinone moieties (Moog et al., 1986). These results point to the value of being able to obtain RR spectra of the underivatized cofactors in quinoproteins.

Resonance Raman spectra have been reported recently for underivatized W3 $MADH_{ox}$ (McIntire et al., 1991a). In the present work we show that the underivatized cofactors in MADHs from *Pd* and *Tv* have almost identical RR spectra, indicating the same cofactor structure in all three proteins. In addition, we have been able to obtain RR spectra for the ammonia and hydroxide adducts of the TTQ cofactor as well as the one-electron-reduced semiquinone form of *Pd* MADH. We find that the different structural states of the quinone-type cofactor are readily distinguished by RR spectroscopy. We have also investigated the RR spectrum of $MADH_{ox}$ in the presence of amicyanin to determine whether either the TTQ or the copper redox site is altered by complex formation. A 2:1 complex of amicyanin and $MADH_{ox}$ has been demonstrated by cocrystallization (Chen et al., 1988) and has been found to alter the electronic spectrum of MADH as well as causing a 73-mV decrease in the redox potential of amicyanin (Gray et al., 1988). However, the RR spectra give no indication of any structural changes in either the TTQ cofactor of MADH or the blue copper site of amicyanin upon complex formation.

Experimental Procedures

Methylamine Dehydrogenase. $MADH_{ox}$ from *P. denitrificans* was purified as described previously (Husain & Davidson, 1987). Isotope exchange was achieved by first diluting 50 μL of ~1 mM MADH to 300 μL with the appropriate buffer in D_2O (Sigma, 99.8 atom %) or $H_2{}^{18}O$ (Cambridge Isotope Laboratories, 97 atom %). The MADH was then concentrated back to 50 μL by centrifugation in a Centricon 30 (Amicon). This cycle was repeated two more times to yield a final concentration of ~1 mM MADH in 0.01 M potassium phosphate (pH meter reading 7.5). The protein samples were then incubated in $H_2{}^{18}O$ (4 days) or D_2O (24 h) at 278 K to ensure complete isotope exchange. In each case the same procedure was performed on a control sample in H_2O at pH 7.5.

The semiquinone form of *Pd* MADH was obtained by addition of 1 mol of dithionite per mole of MADH under anaerobic conditions. The concentration of dithionite was determined from its absorbance at 315 nm, on the basis of $\epsilon = 6900\ M^{-1}\ cm^{-1}$ (Creutz & Sutin, 1974). The sample was frozen in an anaerobic chamber prior to Raman spectroscopy, and the semiquinonoid nature of the sample was verified by absorption spectroscopy following the Raman experiment. The hydroquinone form, $MADH_{red}$, was produced under similar conditions by adding a second equivalent of dithionite. The ammonia adduct was prepared by a series of dilutions and Centricon concentrations (as above) in 10 mM phosphate and 0.4 M NH_4Cl (pH 7.6). The hydroxide adduct at pH 9.0 was prepared by adding concentrated bicine buffer at pH 9.0 to give a 90 mM final buffer concentration.

$MADH_{ox}$ from *T. versutus* was prepared according to van Wielink et al. (1990). The protein was passed through an FPLC Superose column (Pharmacia) containing 50 mM phosphate and 0.2 M NaCl (pH 7.0) and the lyophilized. This material was then dissolved in H_2O, D_2O, or $H_2{}^{18}O$ to yield a final concentration of ~0.8 mM MADH and incubated 24 h at 278 K.

Amicyanin. The blue copper protein from *P. denitrificans* was purified as described by Husain and Davidson (1985).

Spectroscopy. Absorption spectra were recorded on a Perkin-Elmer Lambda 9 spectrophotometer. Fluorescence spectra were obtained on a Perkin-Elmer MPF-66 spectrofluorimeter. Raman spectra were recorded on a Jarrell-Ash 25-300 spectrophotometer equipped with various lasers (Spectra-Physics 164-05 Ar, 2025-11 Kr, Liconix 4050 He/Cd), an RCA C31034 photomultiplier tube, and an ORTEC Model 9302 amplifier and interfaced to an Intel 310 computer. For spectra at 15 K (which yielded the highest quality data), samples were frozen onto a gold-plated sample holder of a closed-cycle helium Displex (Air Products) and illuminated in an ~150° backscattering geometry. For spectra at 278 K (liquid samples required for enhancement profiles), samples were filled in capillaries and inserted in a copper rod cold finger in a Dewar filled with ice. Raman frequencies have been corrected by using an indene standard (Hendra & Loader, 1968) and are accurate to $\pm 1\ cm^{-1}$. All MADH samples were stable to laser irradiation with no indication of photodecomposition under the conditions used. A broad and featureless fluorescence background (that lowers the overall signal-to-noise ratio but has no effect on RR peak positions) has been subtracted.

Results

Comparison of MADH from Different Organisms. Bacterial methylamine dehydrogenases appear to fall into two subclasses (Davidson & Neher, 1987). The proteins from the facultative autotrophic bacteria *Pd* and *Tv* are closely related as shown by the complete immunological cross-reactivity of both subunits. The protein from the methylotrophic bacterium W3 is more distantly related as only its quinone-containing small subunit exhibits cross-reactivity with *Pd* MADH. Similarly, the optical spectra of *Pd* and *Tv* $MADH_{ox}$ more closely match each other with broad maxima centered at 440 nm compared to the narrower band at 429 nm in W3 $MADH_{ox}$ (Table I).

Resonance Raman spectroscopy provides another means for investigating the tryptophylquinone cofactor of MADHs from

Table I: Visible Absorption Bands of Different Forms of Methylamine Dehydrogenase[a]

MADH	quinone	semi-quinone	ammonia adduct[b]	hydroxide adduct[c]
P. denitrificans	440 br	428	425	420
			470 sh	460 sh
T. versutus	440 br		420	424
			480 sh	460 sh
bacterium W3A1[d]	429	428	491	n.o.

[a] Absorption maxima in nanometers (br = broad, sh = shoulder). [b] *P. denitrificans* MADH in 0.01 M PO_4 and 0.4 M NH_4Cl (pH 7.6); *T. versutus* MADH in 0.01 M PO_4 and 0.4 M NH_4Cl (pH 7.0). [c] Samples in 0.01 M bicine buffer (pH 9.0); n.o. = no observable adduct. [d] Data from Kenney and McIntire (1983).

Table II: Raman Vibrational Modes in Methylamine Dehydrogenases from Different Organisms[a]

	Pd MADH				
Tv MADH frozen soln[b]	frozen soln[b]	liquid soln[c]	W3A1 MADH liquid soln[d]		
ν $\Delta^{18}O$	ν $\Delta^{18}O$	ν	ν	$\Delta^{18}O$	ΔD
1634 (−12)	1648 (−6)	1646	1630	(×20)	
*1628 (−22)	*1625 (−16)	*1619	*1614	(−27)	[−3]
1581	1581	1581			
1569	*1570 (−18)	*1564	*1558		[−2]
1527	1531				
1520	1515		1518		[−14]
	1500	1495			
1486	1490	1487	1481		
*1451	*1454	*1452	*1448		[−6]
1385	1381	1378	1371		[+10]
1349	1349	1345	1340		
1307	1305	1306	1300		
1248	1247	1243	1235		
*1163	*1162	*1161	*1157		[+8]
1146	1148	*1148	1140		
1100	1110	1108	1102		
*1062	*1065	*1064	*1059		[−3]
1001	1001	997	997		
944	944	944	941		
	629		659		
	586		580		[−5]
	486 (−5)		486		
	436		443	(−10)	[−10]
	351 (−5)				

[a] Frequencies, ν, in cm^{-1}. $\Delta^{18}O$ = shifts in $H_2{}^{18}O$. ΔD = shifts in D_2O. Peaks of highest intensity are denoted by *. [b] Spectra obtained on frozen solutions at 15 K. [c] Spectra obtained at 278 K. [d] Spectra obtained at 298 K. Data from McIntire et al. (1991a).

different organisms. $MADH_{ox}$ from *Pd* exhibits a characteristic and complex RR spectrum with a series of intense peaks at 1065, 1162, 1454, 1570, and 1625 cm^{-1} (Figure 2A). The many unlabeled smaller peaks are also reproducible spectral features and are well above the noise level. The RR spectrum of $MADH_{ox}$ from *Tv* (Figure 2B) is of poorer quality due to the higher fluorescent background in this protein. Nevertheless, the proteins from the two organisms are very similar, with almost a one-to-one correspondence in peak frequencies and intensities (Table II). All of the frequencies are within 4 cm^{-1} of one another in the two proteins, with the strongest peaks in *Tv* MADH having an *average* difference of −1 cm^{-1} from the values in *Pd* MADH. The *Tv* protein also shows decreased peak intensities at 1500 and 1569 cm^{-1} and increased peak intensities at 977, 1295, 1369, 1412, and 1602 cm^{-1} compared to the *Pd* protein. These small spectral differences are attributed to slight differences in the environments of the TTQ cofactor in the two proteins.

The RR spectrum of W3 $MADH_{ox}$ at 298 K (McIntire et al., 1991a) shows the same pattern of peak intensities as for

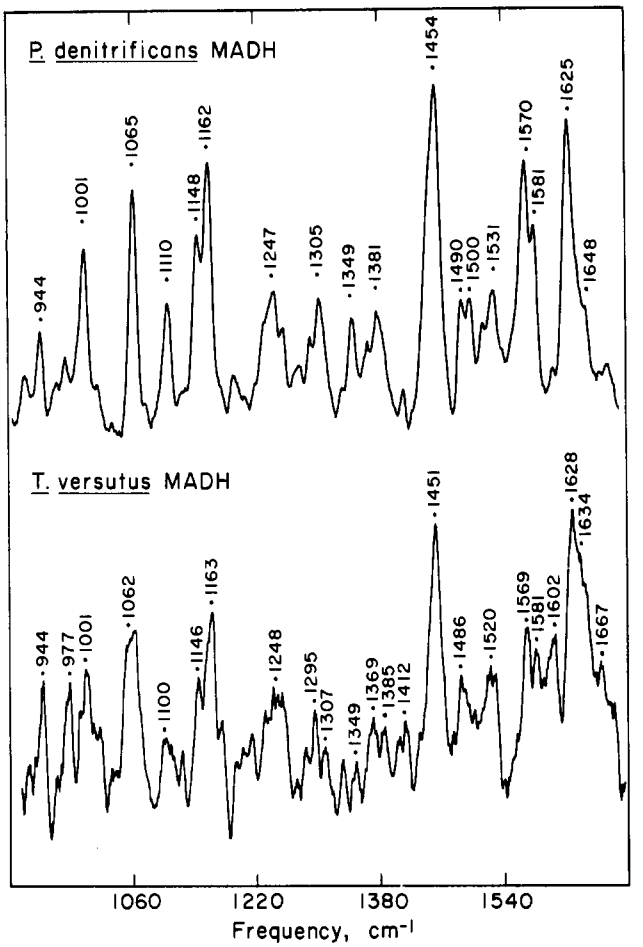

FIGURE 2: Resonance Raman spectra of methylamine dehydrogenase at 15 K. (Upper) *P. denitrificans* $MADH_{ox}$ (1 mM, pH 7.5). (Lower) *T. versutus* $MADH_{ox}$ (0.6 mM, pH 7.0). Spectra were obtained by using 457.9-nm excitation (60 mW) with a resolution of 5 cm^{-1} and a scan rate of 1 cm^{-1}/s, and they represent an accumulation of 16 and 12 scans, respectively.

the *Pd* and *Tv* proteins. A similar set of five intense features occurs at 1059, 1157, 1448, 1558, and 1614 cm^{-1} (Table II). An exact comparison of peak frequencies is complicated by the fact that frozen solids and solutions have slightly different RR frequencies. For *Pd* MADH in solution, the peak frequencies are on the average 3 cm^{-1} lower than at 15 K (Table II). For W3 MADH in solution, the peak frequencies are even lower with an average difference of −5 cm^{-1} from the solution spectrum of Pd MADH (Table II). The average frequency difference for the RR peaks of *Pd* and W3 MADHs is 5 times greater than the −1 cm^{-1} average difference between *Pd* and *Tv* MADHs (discussed above). Nevertheless, it is again more likely due to small differences in cofactor environments (e.g., hydrogen-bond strengths), rather than to structural differences in the cofactors. Dissociation of native W3 MADH into subunits causes a similar degree of change in the RR spectrum of the cofactor with frequencies being +9 cm^{-1} higher on the average in the isolated β-subunit than in the intact enzyme (McIntire et al., 1991a).

Oxygen Isotope Exchange. Studies of PQQ have shown that one of the two quinone carbonyl groups exchanges completely with ^{18}O in the solvent after a 20-h incubation as a result of the reversible hydration and dehydration of the carbonyl moiety (Houck & Unkefer, 1989; Dekker et al., 1982). McIntire et al., (1991a) accomplished carbonyl group exchange of the TTQ cofactor in W3 $MADH_{ox}$ by first forming the ammonia adduct in 0.4 M NH_4Cl and then removing the ammonia in $H_2{}^{18}O$-containing solvent. The RR spectrum of

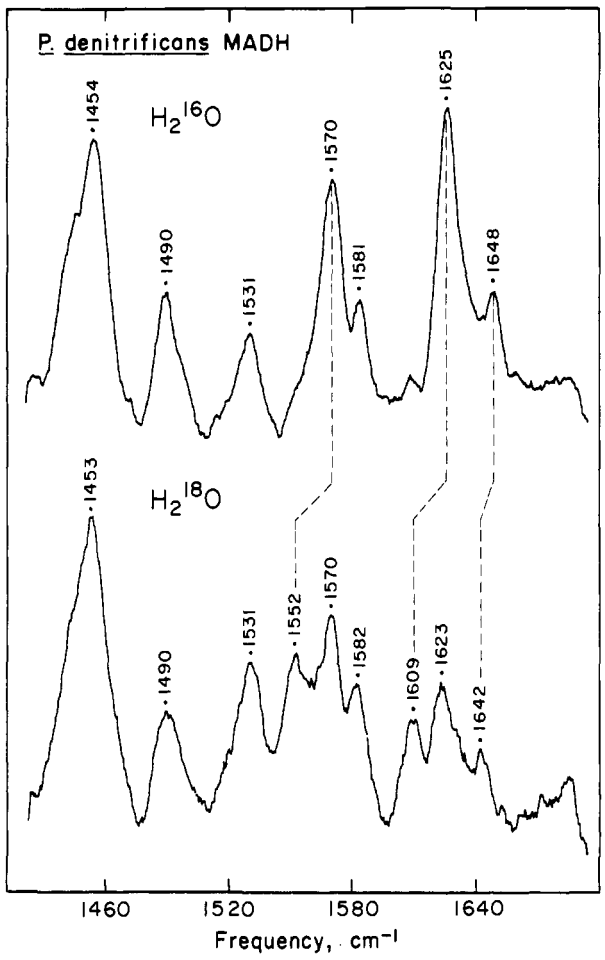

FIGURE 3: Resonance Raman spectra of *Pd* $MADH_{ox}$ equilibrated with $H_2{}^{16}O$ (upper spectrum) and $H_2{}^{18}O$ (lower spectrum). The sample and spectral conditions are the same as in Figure 2 except that spectra represent accumulations of 16 and 25 scans, respectively.

the ^{18}O derivative revealed that the peak at 1614 cm^{-1} underwent a −27 cm^{-1} shift, leading it to be assigned to a C=O stretching vibration. We were able to achieve extensive carbonyl exchange in *Pd* and *Tv* $MADH_{ox}$ solely by incubating the proteins in $H_2{}^{18}O$-containing buffers at neutral pH for 4 days and 24 h, respectively.

Comparison of the RR spectra of ^{18}O- and ^{16}O-equilibrated *Pd* $MADH_{ox}$ samples shows that the 1625-cm^{-1} peak has dropped ~50% in intensity and that a new peak has appeared at 1609 cm^{-1}, corresponding to a 16-cm^{-1} shift to lower energy (Figure 3). The peak at 1628 cm^{-1} in *Tv* MADH undergoes a similar drop in intensity and exhibits a new feature at 1606 cm^{-1}, corresponding to a shift of −22 cm^{-1} in $H_2{}^{18}O$ (Table II). The *Pd* and *Tv* proteins again differ from W3 MADH in the extent of carbonyl oxygen exchange. The W3 MADH exhibits fairly complete exchange as there is very little residual intensity at 1614 cm^{-1} after ^{18}O treatment (McIntire et al., 1991a). Less complete exchange (~50%) occurred with *Pd* MADH, despite the 4-day incubation in $H_2{}^{18}O$. Futhermore, treatment with 0.4 M NH_4Cl + $H_2{}^{18}O$ according to the procedure for W3 MADH (McIntire et al., 1991a) yielded no improvement in the extent of exchange.

Additional ^{18}O shifts are observed for the peaks at 1648 cm^{-1} for *Pd*, at 1634 cm^{-1} for *Tv* and at 1630 cm^{-1} for W3 MADH (Table II). The Raman spectrum of *p*-benzoquinone also shows several ^{18}O-dependent Raman modes in this frequency range whose multiplicity has been attributed to Fermi resonance coupling of the C=O stretch with other vibrational modes (Stammreich & Sans, 1965). There are a few other peaks that show ^{18}O shifts, but these are more variable among the three proteins. In Raman studies of *p*-quinones, a C=O bending mode is typically observed in the 450- to 480-cm^{-1} region, and it exhibits a 10-cm^{-1} shift upon ^{18}O substitution (Stammreich & Sans, 1965; Singh & Singh, 1968). The peak at 486 cm^{-1} in *Pd* MADH decreases by 5 cm^{-1} in $H_2{}^{18}O$ (as is also true for the peak at 351 cm^{-1}), but there is no comparable change in the 486-cm^{-1} band of W3 MADH (Table II). Instead, the 443-cm^{-1} peak of W3 MADH undergoes a 10-cm^{-1} decrease in $H_2{}^{18}O$ whereas the 436-cm^{-1} peak of *Pd* MADH is unaffected. In addition, ~40% of the 1570-cm^{-1} peak in *Pd* MADH is shifted to 1552 cm^{-1} (a change of −18 cm^{-1}) in $H_2{}^{18}O$ (Figure 3). No such ^{18}O-dependence is seen in the ~1570-cm^{-1} peak in *Tv* or W3 MADH. Regardless of these small differences, the three proteins are similar in that the majority of the resonance-enhanced vibrational modes listed in Table II are *not* ^{18}O dependent and, thus, are rather associated with C–C, C–H, and C–N vibrations of the tryptophylquinone moiety.

Deuterium Exchange. Proton-substitution experiments were performed in order to identify vibrational contributions from (i) the NH of the tryptophylquinone and (ii) hydrogen bonds between the protein and the quinone cofactor. Samples of *Pd* and *Tv* $MADH_{ox}$ were incubated in D_2O-containing buffer at neutral pH for 24 h, and the Raman spectra were compared to that of the protein in H_2O. No deuterium shifts of ≥1 cm^{-1} were observed for either protein. This is in marked contrast to the spectra obtained on the W3 protein where the D_2O-equilibrated samples showed a number of substantial changes varying from −14 to +10 cm^{-1} for the peaks at 1518 and 1371 cm^{-1}, respectively (Table II). The downshifts in W3 MADH could be indicative of contributions from tryptophan NH vibrations (Harada & Takeuchi, 1986), whereas the upshifts are more characteristic of hydrogen bonding or Fermi resonance effects (McIntire et al., 1991a). Since no deuterium shifts are observed for either *Pd* or *Tv* MADHs, we conclude that no proton exchange has occurred at either the NH position of the tryptophylquinone or in groups which are hydrogen bonded to it. This suggests that the cofactor in *Pd* and *Tv* MADHs is less accessible to solvent than in W3 MADH.

Raman Enhancement Profiles. Resonance Raman spectral intensities of *Pd* $MADH_{ox}$ in liquid solution were investigated as a function of excitation wavelength by using the 983-cm^{-1} symmetric stretch of sulfate as an internal intensity standard. Data for selected peaks are shown in Figure 4. The excitation profiles indicate that the vibrational modes with frequencies at 1619 and 1064 cm^{-1}, as well as most of the other features in the spectrum, are in resonance with the 440-nm absorption band of the TTQ cofactor. The 1452-cm^{-1} mode shows somewhat different behavior and appears to correspond to electronic transitions at 425 and 500 nm. The presence of multiple electronic transitions is already evident from the breadth and asymmetry of the 440-nm absorption band.

Benzoquinones and related compounds are considered to behave as α-β-unsaturated ketones rather than as aromatic systems (Morton, 1965). Thus, the intense absorption maximum observed between 400 and 480 nm in substituted *o*-benzoquinones has been attributed to a $\pi \rightarrow \pi^*$ transition of the conjugated C=C–C=O moiety. A similar assignment is likely for the 440-nm absorption band in MADH from the fact that the C=O vibrational mode at 1625 cm^{-1} as well as a number of C=C and C–C modes show maximal intensity near 440 nm. The heterocyclic pyrrole ring of the tryptophylquinone moiety would be expected to provide additional pathways for electron delocalization and, thus, help to explain

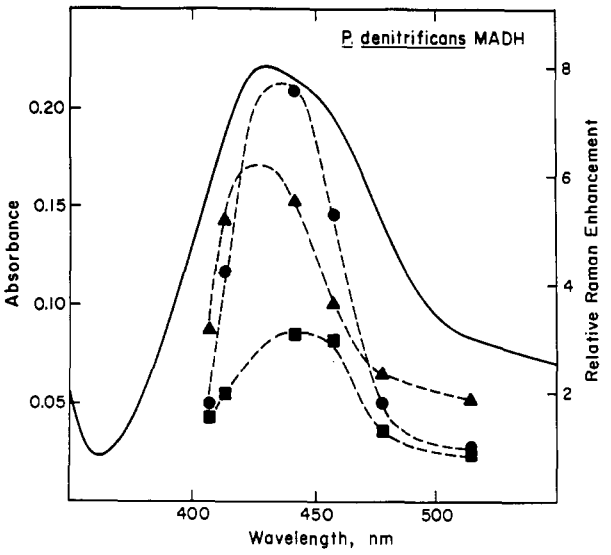

FIGURE 4: Absorption spectrum of *Pd* $MADH_{ox}$ (—) and enhancement profiles (---) for resonance Raman peaks at 1064 (■), 1452 (▲), and 1619 (●) cm^{-1}. Absorption spectrum were obtained on 10 μM MADH in 0.01 M phosphate (pH 7.5). Raman spectra were obtained on 0.3 mM MADH in 0.01 M phosphate and 0.2 M Na_2SO_4 (pH 7.5) at 278 K. The other spectral conditions are the same as in Figure 2. Raman enhancement is calculated from the area of sample peak relative to the area of 983-cm^{-1} sulfate peak. The area of the 1619-cm^{-1} peak includes the shoulder at 1646 cm^{-1}. Enhancement profiles represent the best fit to experimental points from available laser lines.

the multiplicity of electronic transitions associated with this chromophore. In contrast, the tryptophan moiety of TTQ cannot contribute to the 440-nm chromophore because the two indole rings are offset by a dihedral angle of ~45° (Chen et al., 1991) and, thus, are not conjugated. Since the vibrations of an unmodified tryptophan are resonance-enhanced with excitation below 300 nm (Rava & Spiro, 1985; Sweeney & Asher, 1990), they would not be observed in the present experiments using 400- to 500-nm excitation.

Raman Spectrum of MADH Semiquinone. The visible absorption spectrum of the semiquinone, TTQ•, is characterized by a shift in the absorbance maximum from 440 to 428 nm and a 2-fold increase in absorptivity (Husain et al., 1987). Excitation of the semiquinone within its 428-nm absorption band (i.e., at 413.1 nm) generates a Raman spectrum that is quite different from that of $MADH_{ox}$ (Figure 5B). The intense features of the tryptophylquinone spectrum at 1001, 1065, 1148, 1162, ~1500, 1570, and 1625 cm^{-1} are absent or greatly reduced in intensity. The strongest feature in the spectrum of TTQ• is a peak at 1461 cm^{-1}, which has decreased in half-width (i.e., now a single component) compared to the 1454 cm^{-1} peak of the quinone. The peaks at 1364, 1531, and 1538 cm^{-1} are considerably more enhanced than their counterparts in the quinone spectrum.

It is of particular interest that the C=O vibrational mode at 1625 cm^{-1} in $MADH_{ox}$ is no longer observed in the semiquinone (Figure 5B). Carbonyl stretching vibrations in quinones are typically found between 1620 and 1680 cm^{-1} (Gleicher, 1974). The lack of any C=O mode in the RR spectrum of the semiquinone suggests that the C=O moiety is no longer part of the chromophore. As indicated in Figure 6, the radical in TTQ• may be delocalized over C6 (and C7) or further delocalized onto the oxygens or elsewhere on the indole ring. The decreased double bond character of the two carbonyl groups would explain their decreased conjugation with the ring system. The semiquinone is also likely to be deprotonated at neutral pH, on the basis of the fact that pK_a values typically range between 4.0 and 6.2 for the protonation

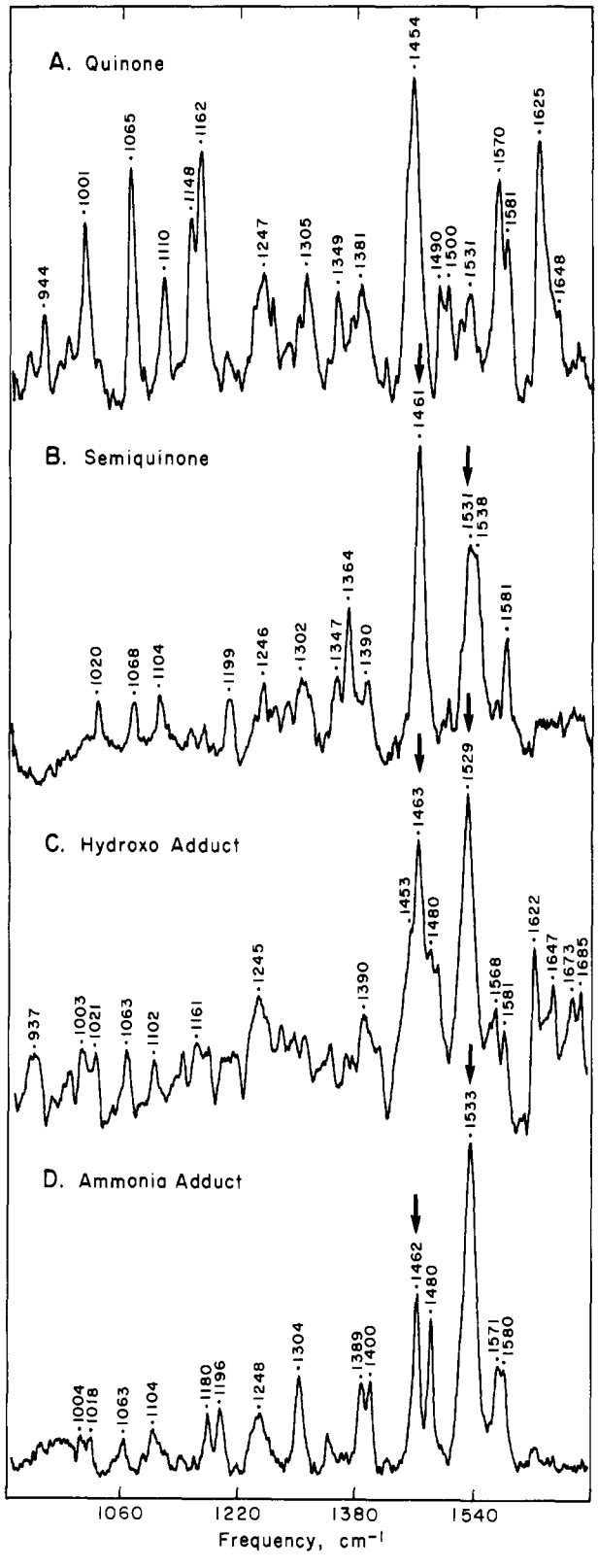

FIGURE 5: Raman spectra of various forms of methylamine dehydrogenase from *P. denitrificans*. (A) $MADH_{ox}$ at pH 7.5, under the same conditions as in Figure 2. (B) Semiquinone form of MADH (0.5 mM) at pH 7.5. (C) MADH (0.5 mM) in 0.09 M bicine buffer (pH 9.0). (D) MADH (0.6 mM) in 0.01 M phosphate and 0.4 M NH_4Cl (pH 7.6). All samples were at 15 K. Spectrum B was obtained with 413.1-nm excitation (20 mW) with 6-cm^{-1} resolution, a 1-cm^{-1}/s scan rate, and 12 scans. Spectra C and D were obtained with 457.9-nm excitation as in Figure 2, but with a resolution of 6 cm^{-1}, and represent accumulations of 15 and 6 scans, respectively. The arrows indicate major spectral features that differ from those of the quinone.

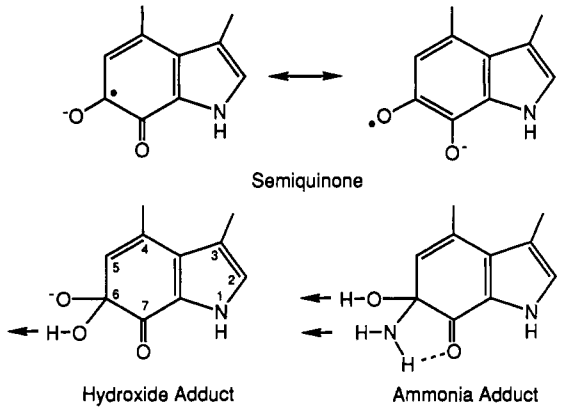

FIGURE 6: Proposed structures for the semiquinone (two of many possible resonance forms shown) and the hydroxide and ammonia adducts of the tryptophylquinone cofactor in MADH. The arrows depict potential hydrogen-bonding interactions with an appropriately positioned carboxylate of Asp 74 in the crystal structure (Chen et al., 1991).

reaction (Swallow, 1982; McWhirter & Klapper, 1990). Since the carbonyl vibrations are essentially independent of the indole ring vibrations, the RR spectral changes in the 1000- to 1660-cm^{-1} region must be due primarily to changes in the indole moiety. The reduced number of resonance-enhanced vibrational modes in TTQ• is another indication of the reduction in the extent of conjugation (e.g., the C–C bonds of the C–C–O moieties have less double bond character). A similar simplification of the RR spectrum has been observed upon reduction of the isoalloxazine ring of FAD or FMN to the semiquinonoid FADH• or FMNH• form (Sugiyama et al., 1985).

Further reduction to $MADH_{red}$, the two-electron-reduced hydroquinone, is accompanied by a complete loss of absorbance in the 420–440-nm region and the appearance of a new absorption band at 330 nm. When $MADH_{red}$ was probed with 350.7-nm excitation (within the 330-nm absorption band), no resonance-enhanced Raman modes could be observed. Use of 413.1-nm excitation produced a weak RR spectrum due to residual semiquinone in the preparation. The failure to obtain a RR spectrum for the $MADH_{red}$ is again reminiscent of the behavior of flavin systems where the $FADH_2$ and $FMNH_2$ forms also fail to produce RR spectra due to the further loss of conjugation (Sugiyama et al., 1985).

Raman Spectra of Ammonia and Hydroxide Adducts. Quinones are known to react with a variety of nucleophilic agents such as water, alcohols, and amines, as has been well-documented in the case of PQQ (Dekker et al., 1982). The tryptophylquinone cofactor of W3 MADH reacts reversibly with ammonia, causing the visible absorption maximum to shift from 429 to 491 nm, and an *iminoquinone* product has been suggested (Kenney & McIntire, 1983). Exposure of *Pd* $MADH_{ox}$ to 0.4 M NH_4Cl also leads to the production of an adduct. However, in this case the absorption maximum shifts to shorter wavelength, from 440 to 425 nm, with a small shoulder at 470 nm. A similar spectral change is observed for *Tv* $MADH_{ox}$ in 0.4 M NH_4Cl (Table I). The ammonia adduct in these two proteins is clearly different from the 491-nm species observed for W3 MADH. The reaction of *Pd* MADH is also reversible. Treatment with 0.4 M NH_4Cl causes an inhibition of enzymatic activity, which is fully restored upon removal of the NH_4Cl by gel filtration (V. L. Davidson and L. H. Jones, unpublished results).

The ammonia adducts of *Pd* and *Tv* MADHs appear to be similar to the pH 9 forms of these two proteins because raising the pH also causes the absorption maximum to shift to shorter wavelength. At pH 9, *Pd* MADH has its major absorption at 420 nm with a shoulder at 460 nm (Davidson, 1989), and *Tv* MADH exhibits corresponding values (Table I). The shift to shorter wavelength in the NH_4Cl and pH 9 treated forms is reminiscent of the spectrum of the MADH semiquinone with its absorption maximum at 428 nm. Thus, it is likely that both ammonia and hydroxide form simple adducts, as shown in Figure 6, which have the consequence of removing one of the carbonyl groups. Addition to the carbonyl group at C-6 is in keeping with the X-ray crystallographic results showing that this is the more accessible carbonyl (Chen et al., 1991).

In the case of PQQ, some of the carbonyl groups are converted to aquo adducts at neutral pH (Dekker et al., 1982), and ionization to the hydroxy form occurs with a pK_a of ~10.7 (Rodriguez et al., 1987). For the TTQ cofactor of MADH, the quinone form appears to predominate at neutral pH with no indication of an aqua adduct in the RR spectrum. The observed pK_a value of 8.2 for the conversion of the 440-nm to the 423-nm species (Davidson, 1989) would then correspond to hydroxide addition. The hydroxide and ammonia adducts of MADH also differ from the corresponding adducts of PQQ in that they result in a decrease rather than an increase in fluorescence (data not shown). This factor is probably responsible for the improvement in Raman spectral quality in Figure 5D.

The resonance Raman spectra of *Pd* MADH provide additional evidence for the structural similarity of the semiquinone, hydroxy, and ammonia forms of TTQ (Figure 5). The hydroxide and ammonia adducts (i) show a similar decrease in the total number of RR modes (including small unlabeled features), (ii) have only two strong RR features at ~1463 and 1530 cm^{-1} instead of the six intense features (at 1001, 1065, 1162, 1454, 1570, and 1625 cm^{-1}) in the RR spectrum of the quinone, and (iii) have a set of similar weaker features at ~1020, 1103, and 1390 cm^{-1}. The decrease in the total number of resonance-enhanced vibrational modes is again ascribed to a decrease in the number of conjugated carbon atoms, as in the case of the semiquinone. The hydroxide adduct has features at 1622 and 1647 cm^{-1} that are likely to be the ν(C=O) modes of residual quinone in the sample. It also has new peaks at 1673 and 1685 cm^{-1}, either of which could be due to ν(C=O) for the single remaining carbonyl group.

The ammonia adduct of *Pd* MADH has no features in the 1600–1750-cm^{-1} region that can be assigned to a C=O stretch. The loss of the ν(C=O) mode is attributed to an alteration of the remaining carbonyl group. In the case of *p*-anthraquinones with hydroxy substituents adjacent to the carbonyl groups, hydrogen bonding appears to be responsible for the lack of resonance enhancement of C=O vibrations in the RR spectrum (Nonaka et al., 1990). It is possible that the ammonia adduct provides an additional hydrogen bond to the C-7 carbonyl group as shown in Figure 6, thereby decreasing its vibrational intensity. An analogous hydrogen bond for the hydroxide adduct may be precluded by interaction of the OH group with the carboxylate of Asp 74, which is in close proximity to the C-6 carbonyl oxygen in the crystal structure (see arrow in Figure 6). Finally, our results indicate that only a single carbonyl group has been modified because addition to both carbonyl groups would produce a hydroquinone-type species that would no longer yield a RR spectrum. Conversely, if the ammonia adduct had been dehydrated to the imine form (as seems likely for W3 MADH) then the RR spectrum would have been more similar to that of the quinone.

MADH Complex with Amicyanin. There are a number of lines of evidence that *Pd* MADH forms a stable electron-transfer complex with its redox partner, amicyanin (Gray et

al., 1988; Kumar & Davidson, 1990). A complex containing two amicyanin per $MADH_{ox}$ (an $\alpha_2\beta_2$ protein) has been crystallized (Chen et al., 1988), and structure determination reveals that the blue copper center of amicyanin is within 10 Å of the TTQ cofactor on the small subunit of MADH (L. Chen, F. S. Mathews, and V. L. Davidson, unpublished results). The interaction of MADH and amicyanin is enhanced at low ionic strength and is accompanied by a shift in redox potential of amicyanin from +294 mV for the free protein to +221 mV in the presence of excess $MADH_{ox}$ (Gray et al., 1988). In view of the sensitivity of MADH and amicyanin to complex formation, we undertook RR studies of *Pd* $MADH_{ox}$ containing a 2–10-fold excess of amicyanin at low ionic strength. We found that the Raman frequencies of $MADH_{ox}$ were totally unaffected by the presence of amicyanin. This indicates that the structure and immediate environment of the TTQ cofactor is unaltered when amicyanin binds to the small subunit of MADH.

We also examined the effect of MADH on the RR spectrum of amicyanin. Amicyanin is a typical cupredoxin in which the copper is coordinated to one cysteine thiolate and two histidine ligands in a trigonal geometry with an axial methionine thioether at a longer distance (Sharma et al., 1988; Adman, 1985). The strong copper–cysteinate interaction is responsible for the appearance of an intense cysteinate → Cu(II) charge transfer transition at 595 nm (ϵ = 4600 M^{-1} cm^{-1}). Excitation within this absorption band yields a set of resonance Raman peaks at 377, 392, 412, and 430 cm^{-1} that are ascribed to the combination of the Cu–S stretching vibration with cysteine ligand deformation modes (Sharma et al., 1988). Similar sets of vibrational modes are observed for all blue copper proteins due to the highly conserved, nearly coplanar, structure of the $Cu–S_\gamma–C_\beta–C_\alpha$ moiety (Han et al., 1991). The RR spectrum of amicyanin shows no alterations in the frequencies or relative intensities of these vibrational modes after treatment with a 3-fold excess of $MADH_{ox}$ (6-fold excess of small subunit). These results suggest that the structure of the copper site and, particularly, the conserved Cys–His ligand binding loop (Han et al., 1991) are unaffected by the binding of MADH to amicyanin. The observed 73-mV drop in the redox potential of amicyanin in the presence of $MADH_{ox}$ (Gray et al., 1988) is more likely related to changes in the protein electrostatic environment upon complex formation.

Discussion

Vibrational Assignments. The RR spectrum of the $MADH_{ox}$ cofactor is characteristic of a quinone. The majority of peaks between 900 and 1600 cm^{-1} are not oxygen-isotope sensitive and, thus, must largely represent C=C, C–C, C–N, and C–H vibrations of the quinone ring. From 1000 to 1260 cm^{-1}, C–H bending modes are likely to predominate as is also the case in the Raman spectra of tryptophan and indole (Harada & Takeuchi, 1986; Takeuchi & Harada, 1986). From 1300 to 1600 cm^{-1}, the major peaks in the MADH spectrum are more likely due to C=, C–C, and C–N stretches. Finally, the MADH peaks in the 1620–1650-cm^{-1} region that are sensitive to ^{18}O-substitution must have C=O stretching character.

The quinone that has been investigated most extensively by vibrational spectroscopy is *p*-benzoquinone. Although there is generally agreement in the assignments of ν(C–C), ν(C=C), and δ(C–H) modes below 1600 cm^{-1}, as originally proposed by Becker et al. (1965), the assignment of ν(C=C) and ν(C=O) stretching modes above 1600 cm^{-1} remains controversial. Stammreich and Sans (1965) found that the peaks at 1690 and 1667 cm^{-1} showed significant shifts to lower energy upon ^{18}O substitution of the quinone (−32 and −66 cm^{-1}, respectively). They assigned the 1690-cm^{-1} mode to ν_{in}(C=O), the in-phase mode of the two carbonyl groups, and the 1667-cm^{-1} mode to a ν(C=C). They ascribed the extensive ^{18}O shift of the latter to Fermi resonance between the high frequency fundamentals (1690 and 1667 cm^{-1}) and combination bands involving pairs of lower frequency fundamentals. Other studies have suggested a reversal of the assignments with ν(C=C) at 1690 and ν(C=O) at 1667 cm^{-1} (Dunn & Francis, 1974; Palmö et al., 1983). Nevertheless, an explanation invoking Fermi resonance is required (Girlando & Pecile, 1979; Kubinyi & Keresztury, 1989). Aside from this Fermi resonance, the two carbonyl groups behave as separate vibrational entities, and their stretching and deformation modes appear to be uncoupled from the vibrations of the atoms in the benzene ring. The Raman spectra of 1,4-naphthoquinone and 9,10-anthraquinone show a similarly complex set of aromatic ring C=C, C–C, and C–H vibrational modes between 900 and 1625 cm^{-1}, with distinct in-phase C=O modes occuring near 1675 cm^{-1} (Singh & Singh, 1968; Nonaka et al., 1990).

For MADH, the ν_{in}(C=O) mode of the two carbonyl groups can be assigned to the RR mode that shows the greatest shift following ^{18}O substitution: 1614 (−27) cm^{-1} for W3, 1625 (−16) cm^{-1} for *Pd*, and 1628 (−22) cm^{-1} for *Tv* MADHs (Table II). Additional ^{18}O-dependent shifts at 1648 (−6) cm^{-1} for *Pd*, at 1634 (−12) cm^{-1} for *Tv*, and at 1630 (~−20) cm^{-1} for W3 MADHs may be accounted for by Fermi resonance coupling. The magnitude of the shift for ν_{in}(C=^{18}O) depends on the number of carbonyl oxygens that have exchanged with solvent oxygen via hydroxide adduct formation. With fully substituted [^{18}O,^{18}O]quinone, a 1625-cm^{-1} ν_{in}(C=O) mode is expected to shift by −38 cm^{-1}, whereas a half-substituted [^{16}O,^{18}O]quinone should shift by only −19 cm^{-1}. For ^{18}O-substituted *p*-benzoquinone, both species were observed and caused the 1686-cm^{-1} ν_{in}(C=O) mode to shift by −32 and −21 cm^{-1}, respectively (Stammreich & Sans, 1965). For the MADHs from *Pd* and *Tv* there is no indication that the ~1625-cm^{-1} carbonyl mode gives rise to two such ^{18}O vibrations (Figure 3, Table II). Furthermore, the observed shift of approximately −20 cm^{-1} is more consistent with a singly exchanged carbonyl group. These findings support the proposed mechanism for hydroxide adduct formation (Figure 6) and the likelihood that one of the two carbonyl groups in MADH is better positioned for substrate attack at the active site of the enzyme (Figure 1).

Semiquinone and Quinone Adducts. The two most striking features in the RR spectrum of the MADH semiquinone compared to the quinone are (i) a decrease in the total number of resonance-enhanced vibrational modes and (ii) a loss of the ν(C=O) mode at 1625 cm^{-1}. The drop in vibrational modes is a consequence of the reduction of the tryptophylquinone ring (Figure 6), which decreases the extent of conjugation as has been similarly described for FAD and FMN radicals (Sugiyama et al., 1985). This change in the nature of the chromophore is most likely to have removed some C–C vibrational modes from the RR spectrum. The reduction of the quinone ring also favors a situation in which the added electron is delocalized over the two carbonyl groups, as shown in Figure 6. Because the CO groups have less participation in the chromophore and less C=O character, they are no longer observed in the RR spectrum.

The hydroxide and ammonia adducts of *Pd* MADH resemble the semiquinone in that they have undergone a similar alteration of the chromophore. In all three cases, there has been a shift of the visible absorption maximum to higher energy (from 440 to ~425 nm), as expected for a decrease in the extent of conjugation. This view is supported by an analogous decrease in the total number of C–C vibrational modes in the RR spectra of the hydroxide and ammonia ad-

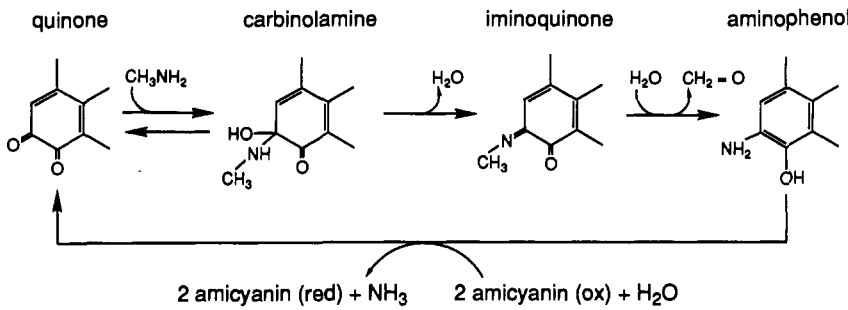

FIGURE 7: Proposed mechanism for MADH oxidation of methylamine to formaldehyde.

ducts (Figure 5). These similarities and the well-known tendencies of quinones to form addition complexes (Duine & Jongejan, 1989; Sleath et al., 1985) led us to propose the structures shown in Figure 6. Although W3 MADH appears to form an unstable amine adduct that dehydrates to the more stable iminoquinone (Kenney & McIntire, 1983), no such dehydration reaction could be confirmed for *Pd* or *Tv* MADHs. An imine compound would have been expected to exhibit a larger number of RR bands in the ν(C–C) and ν(C=C) region with an intensity pattern similar to that of oxidized MADH and a ν(C=O) as well as a ν(C=N) in the 1600–1700-cm^{-1} region. These were not observed.

The ability of MADHs to form hydroxide and ammonia adducts is relevant to the catalytic mechanism of methylamine oxidation and suggests that the amine substrate first adds to the quinone to form a carbinolamine (Figure 7). The accessibility of the two sides of the quinone ring is of interest since enzymes generally favor the attack of substrate at one particular face of a coenzyme (e.g., hydride ion transfer to NAD^+). Similarly, the PQQ-dependent alcohol dehydrogenase from *Pseudomonas testosteroni* selectively binds only one enantiomer of the C-5–acetone adduct at the carbonyl position of PQQ (Jongejan et al., 1989). In the proposed enzymatic mechanism of MADH, the dehydration of the initial amine adduct to an imine requires that amine attack and OH^- release occur on *opposite* faces of the cofactor. This would explain the fairly complete ^{18}O exchange in W3 MADH after cycling through an imine intermediate (McIntire et al., 1991a). The slower rate and lesser extent of ^{18}O exchange in *Pd* and *Tv* MADHs (e.g., only 50% in *Pd* after 4 days of incubation) suggests that addition and release of $^{18}OH^-$ at the C-6 position may be occurring preferentially on the *same* face of the tryptophylquinone ring.

Comparison of MADH from Different Organisms. The TTQ that has been identified as the cofactor in $MADH_{ox}$ from the methylotrophic bacterium W3A1 (McIntire et al., 1991b) has also been proposed to be the cofactor in the MADHs from *P. denitrificans* and *T. versutus*. This analogy is based primarily on fitting of electron density maps for *Pd* and *Tv* MADHs (Chen et al., 1991) and the identification of appropriate tryptophan residues in the DNA sequences for *M. extorquens* AM1 and *Tv* MADHs (Chistoserdov et al., 1990; Ubbink et al., 1991). Resonance Raman spectroscopy provides direct support for this hypothesis. The near identity of the pattern of Raman frequencies and intensities for C–C, C–H, C=C, and C=O vibrational modes *requires that the same tryptophylquinone ring structure be present in all three proteins.* The three MADHs also show similar oxygen-isotope exchange of a single carbonyl oxygen, presumably at the C-6 position (Figure 1).

The MADHs from *Pd* and *Tv* appear to differ significantly from that of W3 with respect to the protein environment of the TTQ cofactor, and these differences have important implications with respect to cofactor reactivity. The environmental effects are clearly observed in the RR spectra where the vibrational frequencies for the tryptophylquinone in *Pd* and *Tv* MADHs differ by an average of only 1 cm^{-1}, whereas the frequencies of *Pd* and W3 MADHs differ by an average of 5 cm^{-1} (Table II). The 5-cm^{-1} higher frequencies in *Pd* MADH could imply stronger tryptophan NH hydrogen bonds to the protein than in W3A1 MADH. This is further substantiated by the quite remarkable differences in the solvent accessibility of the cofactor. The pyrrole NH group of the tryptophylquinone in W3 MADH exchanges with solvent deuterium, yielding dramatic changes in the RR spectrum (Table II). No such deuterium isotope effects are observed in the RR spectra of *Pd* or *Tv* MADHs, indicating that the pyrrole NH is inaccessible to solvent. Similarly, the ν_{in}(C=O) vibration at 1614 cm^{-1} in W3 MADH undergoes a −3 cm^{-1} shift in D_2O that is indicative of hydrogen bonding, whereas no such deuterium isotope effect on ν_{in}(C=O) is observed for either *Pd* or *Tv* MADHs (Table II). Yet the crystal structures of the latter two proteins indicate that both the N-1 amine and the C-7 carbonyl are hydrogen bonded to the protein (Figure 1). The failure of *Pd* and *Tv* MADHs to exhibit hydrogen exchange implies a more rigid polypeptide structure in the vicinity of the TTQ cofactor.

The two classes of MADH also show surprising differences in cofactor reactivity toward hydroxide and ammonia. The MADHs from *Pd* and *Tv* form hydroxide adducts at pH 9 that are readily detected by absorption and RR spectroscopy (Table I, Figure 5). No such hydroxide adduct is apparent for W3 MADH at pH 9.2 (McIntire et al., 1991a), suggesting that cofactor dehydration is favored over hydration in this protein. The MADHs from *Pd* and *Tv* both react with ammonia to yield a carbinolamine (Figure 6) that has absorption (λ_{max} = 425 nm) and RR spectroscopic properties similar to those of the hydroxide adducts. The W3 MADH forms a different type of adduct with ammonia on the basis of its absorption spectrum (λ_{max} = 491 nm) and its photolability (no RR spectrum); it is likely to be the iminoquinone dehydration product (McIntire et al., 1991a). These differences in reactivity toward ammonia may help to explain why ammonium ion has an activating effect on the enzymatic activity of W3 MADH (Kenney & McIntire, 1983) but has no such activating effect with *Pd* or *Tv* MADHs.

CONCLUSIONS

(1) The RR spectrum of MADH provides a distinctive fingerprint of the TTQ cofactor. The same cofactor is present in the W3 MADH utilized for the chemical identification of TTQ and in the *Pd* and *Tv* MADHs utilized for the crystallographic identification of TTQ.

(2) RR spectra show that neither the TTQ site in *Pd* MADH nor the blue copper site in *Pd* amicyanin (its electron-transfer partner) are structurally perturbed by the protein–protein interaction. The change in the redox potential of amicyanin is attributed to electrostatic interactions accompanying complex formation.

(3) In contrast, marked RR spectral changes occur upon

reduction to the semiquinone or upon addition of hydroxide or ammonia to *Pd* MADH. The similarity of the spectra in these three cases derives from the decreased conjugation of the TTQ cofactor.

(4) Reaction with ammonia to form the carbinolamine adduct is also observed for *Tv* MADH but differs from W3 MADH, which dehydrates to the iminoquinone. These differences in cofactor reactivity may explain why W3 MADH responds to ammonia as an activator, whereas *Pd* and *Tv* MADHs do not.

Added in Proof

The $\sim$1625-cm^{-1} frequency for the in-phase C=O stretch of the tryptophylquinone in MADH is markedly lower than the typical quinone value of $\sim$1675 cm^{-1} (Singh & Singh, 1968; Nonaka et al., 1990). The low energy of this vibrational mode is most likely due to strong hydrogen bonding and is consistent with the crystallographic observation that one or both of the cofactor oxygens are hydrogen bonded in MADH (Chen et al., 1991). A similar type of C=O bond polarization has been detected in an enzyme-bound intermediate of lactate dehydrogenase where the 34 cm^{-1} decrease in ν(C=O) of pyruvate has also been ascribed to hydrogen bonding of the carbonyl oxygen (Deng et al., 1989).

Acknowledgments

We thank Dr. Thomas M. Loehr for a critical reading of the manuscript, Drs. William S. McIntire and David M. Dooley for providing copies of manuscripts prior to publication, and Limei Hsu Jones for technical assistance.

References

Adman, E. T. (1985) in *Metalloproteins* (Harrison, P., Ed.) Part 1, pp 1–42, Verlag Chemie, Weinheim, FRG.

Becker, E. D., Charney, E., & Anno, T. (1965) *J. Chem. Phys. 42*, 942–949.

Brown, D. E., McGuirl, M. A., Dooley, D. M., Janes, S. M., Mu, D., & Klinman, J. P. (1991) *J. Biol. Chem. 266*, 4049–4051.

Carey, P. R. (1982) *Biochemical Applications of Raman and Resonance Raman Spectroscopies*, p 47, Academic Press, New York.

Chen, L., Lim, L. W., Mathews, F. S., Davidson, V. L., & Husain, M. (1988) *J. Mol. Biol. 203*, 1137–1138.

Chen, L., Mathews, F. S., Davidson, V. L., Huizinga, E., Vellieux, F. M. D., Duine, J. A., & Hol., W. G. J. (1991) *FEBS Lett. 287*, 163–166.

Chistoserdov, A. Y., Tsygankov, Y. D., & Lidstrom, M. E. (1990) *Biochem. Biophys. Res. Commun. 172*, 211–216.

Creutz, C., & Sutin, N. (1974) *Inorg. Chem. 13*, 2041–2043.

Davidson, V. L. (1989) *Biochem. J. 261*, 107–111.

Davidson, V. L., & Neher, J. W. (1987) *FEMS Microbiol. Lett. 44*, 121–124.

de Beer, R., Duine, J. A., Frank-Jzn, J., & Large, P. G. (1980) *Biochim. Biophys. Acta 622*, 370–374.

Dekker, R. H., Duine, J. A., Frank-Jzn, J., Verwiel, P. E. J., & Westerling, J. (1982) *Eur. J. Biochem. 125*, 69–73.

Deng, H., Zheng, J., Burgner, J., & Callender, R. (1989) *Proc. Natl. Acad. Sci. U.S.A. 86*, 4484–4488.

Duine, J. A., & Jongejan, J. A. (1989) *Annu. Rev. Biochem. 58*, 403–426.

Dunn, T. M., & Francis, A. H. (1974) *J. Mol. Spectrosc. 50*, 1–7.

Girlando, A., & Pecile, C. (1979) *J. Mol. Spectrosc. 77*, 374–384.

Gleicher, G. J. (1974) in *The Chemistry of Quinoid Compounds* (Patil, S., Ed.) pp 1–36, John Wiley, New York.

Gray, K. A., Davidson, V. L., & Knaff, D. B. (1988) *J. Biol. Chem. 263*, 13987–13990.

Han, J., Loehr, T. M., Freeman, H. C., Codd, F., Huq, L., Beppu, T., Adman, E. T., & Sanders-Loehr, J. (1991) *Biochemistry* (in press).

Harada, I., & Takeuchi, H. (1986) in *Spectroscopy of Biological Systems* (Clark, R. J. H., & Hester, R. E., Eds.) pp 113–175, John Wiley, London.

Hartman, C., & Klinman, J. P. (1988) *Biofactors 1*, 41–49.

Hendra, P. J., & Loader, E. J. (1968) *Chem. Ind. (Duesseldorf)*, 718–719.

Houck, D. R., & Unkefer, C. J. (1989) in *PQQ and Quinoproteins* (Jongejan, J. A., & Duine, J. A., Eds.) pp 256–258, Kluwer Academic Publishers, Dordrecht, The Netherlands.

Husain, M., & Davidson, V. L. (1985) *J. Biol. Chem. 260*, 14626–14629.

Husain, M., & Davidson, V. L. (1987) *J. Bacteriol. 169*, 1712–1717.

Husain, M., Davidson, V. L., Gray, K. A., & Knaff, D. B. (1987) *Biochemistry 26*, 4139–4143.

Ishii, Y., Hase, T., Fukumori, Y., Matsubara, H., & Tobari, J. (1983) *J. Biochem. 93*, 107–119.

Janes, S. M., Mu, D., Wemmer, D., Smith, A. J., Kaur, S., Maltby, D., Burlingame, A. L., & Klinman, J. P. (1990) *Science 248*, 981–987.

Jongejan, J. A., Groen, B. W., & Duine, J. A. (1989) in *PQQ and Quinoproteins* (Jongejan, J. A., & Duine, J. A., Eds.) pp 205–215, Kluwer Academic Publishers, Dordrecht, The Netherlands.

Kenney, W. C., & McIntire, W. C. (1983) *Biochemistry 22*, 3858–3868.

Kubinyi, M., & Keresztury, G. (1989) *Spectrochim. Acta 45A*, 421–429.

Kumar, M. A., & Davidson, V. L. (1990) *Biochemistry 29*, 5299–5304.

McIntire, W. S., & Stults, J. T. (1986) *Biochem. Biophys. Res. Commun. 141*, 562–568.

McIntire, W. S., Bates, J. L., Brown, D. E., & Dooley, D. M. (1991a) *Biochemistry 30*, 125–133.

McIntire, W. S., Wemmer, D. E., Chistoserdov, A. Y., & Lidstrom, M. E. (1991b) *Science 252*, 817–824.

McWhirter, R. B., & Klapper, M. H. (1990) *Biochemistry 29*, 6919–6926.

Moog, R. S., McGuirl, M. A., Cote, C. E., & Dooley, D. M. (1986) *Proc. Natl. Acad. Sci. U.S.A. 83*, 8435–8439.

Morton, R. A. (1965) in *Biochemistry of Quinones* (Morton, R. A., Ed.) Chapter 2, Academic Press, New York.

Nishimura, Y., Hirakawa, A. Y., & Tsuboi, M. (1978) in *Advances in Infrared and Raman Spectroscopy* (Clark, R. J. H., & Hester, R. E., Eds.) Vol. 5, pp 217–275, Heyden, London.

Nonaka, Y., Tsuboi, M., & Nakamoto, K. (1990) *J. Raman Spectrosc. 21*, 133–141.

Palmö, K., Pietilä, L.-O., Mannfors, B., Karonen, A., & Stenman, F. (1983) *J. Mol. Spectrosc. 100*, 368–376.

Rava, R. P., & Spiro, T. G. (1985) *J. Phys. Chem. 89*, 1856–1861.

Rodriguez, E. J., Bruice, T. C., & Edmondson, D. E. (1987) *J. Am. Chem. Soc. 109*, 532–537.

Sharma, K. D., Loehr, T. M., Sanders-Loehr, J., Husain, M., & Davidson, V. L. (1988) *J. Biol. Chem. 263*, 3303–3306.

Singh, S. N., & Singh, R. S. (1968) *Spectrochim. Acta 24A*, 1591–1597.

Sleath, P. R., Noar, J. B., Eberlein, B. A., & Bruice, T. C. (1985) *J. Am. Chem. Soc. 107*, 3328–3338.

Stammreich, H., & Sans, T. T. (1965) *J. Chem. Phys. 42*, 920–931.

Sugiyama, T., Nisimoto, Y., Mason, H. S., & Loehr, T. M.

(1985) *Biochemistry 24*, 3012–3019.
Swallow, A. J. (1982) in *Function of Quinones in Energy Conserving Systems* (Trumpower, B. L., Ed.) pp 59–72, Academic Press, New York.
Takeuchi, H., & Harada, I. (1986) *Spectrochim. Acta 42A*, 1069–1078.
Ubbink, M., van Kleef, M. A. G., Kleinjan, D.-J., Hoitink, C. W. G., Huitema, F., Beintema, J. J., Duine, J. A., & Canters, G. W. (1991) *Eur. J. Biochem.* (in press).
van der Meer, R. A., Jongejan, J. A., & Duine, J. A. (1987) *FEBS Lett. 221*, 299–304.
van Wielink, J. E., Frank-Jzn, J., & Duine, J. A. (1990) *Methods Enzymol. 188*, 235–241.
Vellieux, F. M. D., Huitema, F., Groendijk, H., Kalk, K. H., Frank-Jzn, J., Jongejan, J. A., Duine, J. A., Petratos, K., Drenth, J., & Hol, W. G. J. (1989) *EMBO J. 8*, 2171–2178.

Iron Binding to Horse Spleen Apoferritin: A Vanadyl ENDOR Spin Probe Study†

Phillip M. Hanna,‡ N. Dennis Chasteen,*,‡ Gerald A. Rottman,§ and Philip Aisen*,§

Department of Chemistry, University of New Hampshire, Durham, New Hampshire 03824, and Department of Physiology and Biophysics, Albert Einstein College of Medicine, 1300 Morris Park Avenue, Bronx, New York 10461

Received May 24, 1991; Revised Manuscript Received July 8, 1991

ABSTRACT: The role of the protein shell in the formation of the hydrous ferric oxide core of ferritin is poorly understood. A VO^{2+} spin probe study was undertaken to characterize the initial complex of Fe^{2+} with horse spleen apoferritin (96% L-subunits). A competitive binding study of VO^{2+} and Fe^{2+} showed that the two metals compete 1:1 for binding at the same site or region of the protein. Curve fitting of the binding data showed that the affinity of VO^{2+} for the protein was 15 times that of Fe^{2+}. Electron nuclear double resonance (ENDOR) measurements on the VO^{2+}–apoferritin complex showed couplings from two nitrogen nuclei, tentatively ascribed to the N1 and N3 nitrogens of the imidazole ligand of histidine. The possibility that the observed nitrogen couplings are from two different ligands is not precluded by the data, however. A pair of exchangeable proton lines with a coupling of approximately 1 MHz is tentatively assigned to the NH proton of the coordinated nitrogen. A 30–40% reduction in the intensity of the ^1H matrix ENDOR line upon D_2O–H_2O exchange indicates that the metal-binding site is accessible to solvent and, therefore, to molecular oxygen as well. The ENDOR data provide the first evidence for a principle iron(II)-binding site with nitrogen coordination in an L-subunit ferritin. The site may be important in Fe^{2+} oxidation during the beginning stages of core formation.

From microorganisms to man, ferritin plays a central role in the biological management of iron (Ford et al., 1984; Clegg et al., 1980a; Crichton, 1973; Thiel, 1987, 1989). The protein consists of a hollow spherical protein shell of 24 nearly identical subunits encapsulating a hydrous ferric oxide mineral core (Ford et al., 1984). Ferritins consist of so called H (heavy) and L (light) subunits with similar molecular weights (ca. 20000) but slightly different mobilities on SDS–PAGE. There is 60–65% sequence homology between the two types of subunits (Theil, 1989). The horse spleen protein used in the present work consists of 96% L-subunits.

Eight hydrophilic and six hydrophobic channels penetrate the protein shell along 3-fold and 4-fold symmetry axes, respectively (Ford et al., 1984). The hydrophilic channels have been generally thought to be the ports through which iron enters and leaves the protein interior but recent work with recombinant H-chain ferritins has called this idea into question (Treffry et al., 1989). During deposition, iron enters the protein as Fe^{2+} and is subsequently oxidized to Fe^{3+}, becoming incorporated into the mineral core (Bryce & Crichton, 1973). In horse spleen apoferritin, Fe^{2+} binding and oxidation appear to be protein-assisted in the early stage of core development (Crichton & Roman, 1978; Paques et al., 1979). After sufficient core has developed, oxidation and deposition appears to occur directly on the growing mineral surface (Macara et al., 1972; Clegg et al., 1980a,b). An important "ferroxidase" site has recently been identified in human liver H-subunit apoferritin by using genetically engineered mutant proteins (Lawson et al., 1989, 1991; Levi et al., 1988, 1989). To date no such site has been identified on an L-subunit although L-subunit rich horse spleen ferritin is competent in oxidizing and storing iron.

The vanadyl ion is a useful paramagnetic probe of metal-binding sites in biological systems (Chasteen, 1981, 1983) and has been used in previous in vitro studies of apoferritin (Wardeska et al., 1986; Chasteen & Theil, 1982). Vanadyl complexes with ferritin are also of interest since they are known to occur in tissues of rats raised on a vanadium-supplemented diet (Chasteen et al., 1986a,b). In vitro room temperature EPR studies at pH 6.25 and 7.0 suggest that vanadyl binding in apoferritin occurs at or near sites that also bind Fe^{2+} and Fe^{3+} (Wardeska et al., 1986; Chasteen & Theil, 1982). Therefore, it appears that the vanadyl ion binds at one or more sites involved in iron accumulation in ferritin and may be used as a spectroscopic and mechanistic probe of these sites.

EPR spin Hamiltonian parameters suggest that the ligation about the bound VO^{2+} in apoferritin consists primarily of O-donor ligands (Chasteen, 1981; Chasteen & Theil, 1982). The vanadyl (d^1) unpaired electron occupies a nonbonding d_{xy} orbital in the ground state, resulting in ligand electron–nuclear hyperfine interactions that are generally too small to be observed in the EPR spectrum. These interactions may be measured, however, by electron–nuclear double resonance (ENDOR) spectroscopy.

† This work was supported by Grants 2 RO1 GM20194 (N.D.C.), 2 RO1 DK15056 (P.A.), and 1 K11 DK01841 (G.A.R.) from the National Institutes of Health.
* Authors to whom correspondence should be addressed.
‡ University of New Hampshire.
§ Albert Einstein College of Medicine.

0006-2960/91/0430-9210$02.50/0